Finite Difference Method for Biaxial and Uniaxial Buckling of Rectangular Silver Nanoplates Resting on Elastic Foundations in Thermal Environments Based on Surface Stress and Nonlocal Elasticity Theories

M. Karimi [*], A.R. Shahidi

Department of Mechanical Engineering, Isfahan University of Technology, Isfahan, Iran

ABSTRACT

In this article, surface stress and nonlocal effects on the biaxial and uniaxial buckling of rectangular silver nanoplates embedded in elastic media are investigated using finite difference method (FDM). The uniform temperature change is utilized to study thermal effect. The surface energy effects are taken into account using the Gurtin-Murdoch's theory. Using the principle of virtual work, the governing equations considering small scale for both nanoplate bulk and surface are derived. The influence of important parameters including, the Winkler and shear elastic moduli, boundary conditions, in-plane biaxial and uniaxial loads, and width-to-length aspect ratio, on the surface stress effects are also studied. The finite difference method, uniaxial buckling, nonlocal effect for both nanoplate bulk and surface, silver material properties, and below-mentioned results are the novelty of this investigation. Results show that the effects of surface elastic modulus on the uniaxial buckling are more noticeable than that of biaxial buckling, but the influences of surface residual stress on the biaxial buckling are more pronounced than that of uniaxial buckling.

© 2016 IAU, Arak Branch.All rights reserved.

Keywords : Biaxial and uniaxial buckling; Surface stress theory; Finite difference method; Thermal environment; Nonlocal elasticity theory.

1 INTRODUCTION

TODAY, nano science and nanotechnology are a field of research that is rapidly progressing and being inclusive. Nano scale structures such as nanoplates, nanobeams and nanotubes are cells of nano structures. Thus, many fields of science and engineering are working in nanotechnology. Recently, there is extremely interest to expanding micro/nanomechanical and micro/nanoelectromechanical systems (MEMS/NEMS), such as sensors, switches, actuators, and so on. These devices can be contributed to novel technological developments in many fields industry [1]. So far, three main methods have been presented for studying mechanical behaviors of nanostructures. These include atomistic [2,3], semi-continuum [4], and classical continuum models [5,6]. However, both the atomistic and semi-continuum hypothesizes are computationally expensive and are not suitable for investigating macroscale systems. Thus, the continuum mechanics are immensely preferred due to their simplicity. The important

_____
[*]Corresponding author. Tel.: +98 3113915237; Fax: +98 3113915216.
E-mail address: morteza.karimi@me.iut.ac.ir (M.Karimi).

feature of nano structures is their high surface-to-volume ratio, which makes elastic response of their surface layers to be different from macroscale structures. Therefore, Gurtin and Murdoch [7,8] expanded a theory based on continuum mechanics that included the effects of surface layers. In this situation the surfaces were modeled as a mathematical layers with zero thickness that they had own properties. These properties affect on physical, mechanical, and electrical properties as well as mechanical response of the nanostructure. For example, Assadi et al. [9] and Assadi [10] studied free and forced vibration of nanoplates considering surface stress effects. Moreover, Assadi and Farshi [11,12] investigated surface stress effects on the vibration and buckling of circular nanoplate. They reported that surface energy effects had important effects on the nanostructures. In addition, increasing in the thickness of nanoplate cause decreasing of the surface energy effects. Gheshlaghi and Hasheminejad [13] and Nazemnezhad et al. [14] analyzed surface stress effects on nonlinear free vibration of nanobeams. They showed that the effect of the surface density on the variation of the natural frequency of the nanobeam versus the thickness ratio could decreases consistently with the increase of the mode number. Hashemi and Nazemnezhad [15], and Sharabiani and Haeri Yazdi [16] investigated nonlinear free vibrations of functionally graded nanobeams with surface energy effects. They demonstrated that by increasing in functionally graded nanobeam dimensions, the surface stress effects on nonlinear natural frequency would decrease. Ansari and Sahmani [17] analyzed bending and buckling behavior of nanobeams by including surface stress effects and normal stresses, utilising different beam theories. They indicated that the distinguishing between the behaviors of nanobeams predicted by with and without surface stress effects were dependent on the magnitudes of the surface elastic constants. In these works [9-17], because of using Navier's method, the above-mentioned researchers were not able to study other boundary conditions.

Karimi et al. [18] investigated free vibration analysis of rectangular nanoplates including surface energy effects using finite difference method (FDM). They reported that the effects of surface properties were amenable to diminish in thicker nanoplates, and vice versa. Challamel and Elishakoff [19] studied the buckling of nanobeams, incorporating the surface stress into the Euler–Bernoulli and Timoshenko theories. They explained that the surface effects may soften a nanostructure for some specific boundary condition. Park [20] studied surface stress effects on the critical buckling strains of silicon nanowires. He indicated that accounting for axial strain relaxation due to surface stresses may be necessary to improve the accuracy and predictive capability of analytic linear surface elastic theories. Recently, Ansari et al. [21] studied surface energies on the buckling, and maximum deflection of nanoplates utilizing first order shear deformation theory and generalized differential quadrature method (GDQM). Moreover, they [22] investigated forced vibration of nanobeams based on the surface stress elasticity and Timoshenko beam theories using GDQM.They indicated that the significance of surface elasticity effects on the response of nanoplate were dependent on its size, type of edge supports, and the selected surface constants. In addition, Mouloodi et al. [23,24] analyzed the surface energy effects on the bending and vibration of multi layered nanoplate. In addition, Wang and Wang [25] investigated the surface stress effects on the bending and vibration of Mindlin nanoplates. In these works [23-25], the finite element model was used to solve governing equations via classical beam and plate theories. They showed that the deflections and frequencies of nanoplates had a dramatic dependence on the surface stress effects. In these works [9-25], the effect of nonlocal parameter was not considered. Due to the presto expansion of technology, especially in micro- and nano-scale fields, one must consider small scale effects to obtain solutions with acceptable precision. Neglecting these effects in some cases may result in completely incorrect methods, and consequently wrong designs. Therefore, in nanoscale, the small scale effects cannot be neglected. For this reason, some researchers investigated the surface influences on the buckling and vibration, including small scale effect. For example, Wang and Wang [26, 27] analyzed buckling and vibration of nanoplates combining both surface layer model and nonlocal elasticity using Navier's method. They showed that by raising the value of nonlocal parameter, the surface elasticity effects could decrease. Farajpour et al. [28,29] investigated the surface energy and nonlocal effects on the buckling and vibration of circular graphene sheets using DQM. They studied only clamped boundary condition. It was shown that the size effects would decrease with an augmenting in the degree of surface residual tensions. In these works [26-29], the small scale effects were only considered for the bulk of nanoplates.

Juntarasaid et al. [30] analyzed the bending and buckling of nanowires, including the effects of surface stress and nonlocal elasticity. They showed that nanowires including both effects appear in-between; i.e., one of nanowires with surface stress and the one with nonlocal elasticity. Mahmoud et al. [31, 32] analyzed the bending and vibration of nanobeams, including surface and nonlocal effects. They reported that the nonlocal effect on the deflection was significant, practically for a smaller thickness. Moreover, by increasing the nonlocal parameter the deflection of nanobeams would increase. Recently, Karimi et al. [33] Combined surface energy effects and nonlocal refined plate theories on the buckling and vibration of rectangular nanoplates utilising DQM. They showed that the nonlocal effects on the shear buckling and vibration are more remarkable than that of biaxial buckling and vibration. Hosseini Hashemi et al. [34] studied the vibration of nanobeams, incorporating the surface stress into the Euler–Bernoulli and

Timoshenko theories. They reported that considering rotary inertia and shear deformation had more effect on the surface effects than the nonlocal parameter. In these works [30-34], the effects of small scale were considered for both nanoplate bulk and surface.

In recent years, Ghorbanpour Arani et al. [35] analyzed nonlocal surface piezoelasticity theory for dynamic stability of double-walled boron nitride nanotube conveying viscose fluid based on different theories. Moreover, they [36] investigated nonlinear surface energy and nonlocal piezoelasticity theories for vibration of embedded single-layer boron nitride sheet using harmonic differential quadrature and differential cubature methods. They [35-36] indicated that neglecting the surface stress effects, the difference between dynamic instability regions of three theories becomes remarkable.

Recently, Mohammadi et al. [37-39] and Asemi et al. [40] investigated uniform temperature influences effects on the vibration and buckling of rectangular, circular and annular graphene sheets based on nonlocal hypothesis without considering surface stress effects. They represented that the effect of temperature change on the vibration becomes the opposite at higher temperature case in compression with the lower temperature case.

In recent years, Ghorbanpour Arani et al. [41] studied 2d-magnetic field and biaxiall in-plane pre-load effects on the vibration of double bonded orthotropic graphene sheets using DQM. In addition, Ghorbanpour Arani and Amir [42] investigated nonlocal vibration of embedded coupled CNTs conveying fluid under thermo-magnetic fields via Ritz method. They reported that results of this investigation could be applied for optimum design of nano/micro mechanical devices for controlling stability of coupled systems conveying fluid under thermo-magnetic fields. Recently, Ghorbanpour Arani et al. [43] analyzed nonlocal DQM for large amplitude vibration of annular boron nitride sheets on nonlinear elastic medium. They showed that with increasing nonlocal parameter, the frequency of the coupled system becomes lower. Moreover, Anjomshoa et al. [44] studied frequency analysis of embedded orthotropic circular and elliptical micro/nano-plates using finite element method (FDM) considering nonlocal elasticity. They indicated that the natural frequencies depend on the non-locality of the micro/nano-plate, especially at small dimensions. Naderi and Saidi [45] analyzed nonlocal postbuckling analysis of graphene sheets in a nonlinear polymer medium. In addition, they [46] investigated modified nonlocal Mindlin plate theory for buckling analysis of nanoplates. They reported that variation of buckling load versus the mode number was physically acceptable. In these works [41-46], the effects of surface energy were not considered.

The main objective of this article is to numerically investigate buckling of rectangular silver nanoplates. In the present work, surface energy and nonlocal effects on the biaxial and uniaxial buckling of rectangular silver nanoplates embedded in elastic media are studied using FDM**.** Small-scale and surface elasticity effects are introduced using the Eringen's nonlocal elasticity and Gurtin-Murdoch's theory, respectively. The governing equations are derived from the principle of virtual displacements. Using this principle, the nonlocal governing equations for both nanoplate bulk and surface are derived. FDM is used to solve the governing equations for simply-supported and clamped boundary conditions together with their various combinations. To validate the accuracy of the FDM solutions, the governing equations are also solved by the Navier's method. The influence of important parameters including, the Winkler and shear elastic moduli, boundary conditions, in-plane biaxial and uniaxial loads, and width-to-length aspect ratio, on the surface stress effects are also studied and discussed.

2   NONLOCAL PLATE MODEL WITH SURFACE ENERGY AND THERMAL EFFECTS

By using nonlocal elasticity theory [47] and disregarding body forces, the stress equilibrium equation for a linear homogeneous nonlocal elastic body can be written as:

$$\sigma_{ij}^{nl} = \int \zeta(|x - x'|, \psi) C_{ijkl} \varepsilon_{kl}(x') dV(x') \quad \forall x \in V \tag{1}$$

Here, $\sigma_{ij}^{nl}, \varepsilon_{ij}$ and C_{ijkl} are the stress, strain and fourth-order elasticity tensor, respectively. $\zeta(|x - x'|, \psi)$ is regarded as a nonlocal modulus, $|x - x'|$ represents a Euclidean distance and γ is a material constant ($\psi = e_0 a_0 / l$) depending on the internal characteristics length, a and external characteristic length, l. Parameter a_0 is a lattice parameter, granular size, or the distance between C–C bonds. Parameter e_0 is estimated such that relations of nonlocal elasticity model could provide satisfactory atomic dispersion curves of plane waves by using approximations from atomic lattice dynamics. Since a constitutive law of integral form is difficult to implement, a simplified differential form of Eq. (1) is used as the basis:

$$(1-g^2\nabla^2)\sigma_{ij}^{nl} = C_{ijkl}\,\varepsilon_{kl} \tag{2}$$

In the above equation, $\nabla^2 = \left(\partial^2/\partial x^2\right)+\left(\partial^2/\partial y^2\right)$ is the Laplacian. $g^2 = \left(e_0 a_0\right)^2$ is the nonlocal parameter. The displacement components in the x, y, and z directions are obtained from the Kirchhoff's plate model, as follows [18]:

$$u_x(x,y,z) = u_0(x,y) - z\frac{\partial w(x,y)}{\partial x}, \quad u_y(x,y,z) = v_0(x,y) - z\frac{\partial w(x,y)}{\partial y}, \quad u_z(x,y,z) = w(x,y) \tag{3}$$

where u_0, v_0, and w are axial and transverse displacements of any point on mid-plane. Since the axial displacements at the mid-plane (u_0, v_0) have a very small effect, they are neglected for the current analysis. The resulting strain components in the Cartesian coordinates can be derived by using the relations of Eq. (3), which are always considered to be the same for both nanoplates bulk and surface [18]:

$$\varepsilon_{xx} = -z\frac{\partial^2 w}{\partial x^2} \;,\; \varepsilon_{yy} = -z\frac{\partial^2 w}{\partial y^2} \;,\; \gamma_{xy} = -2z\frac{\partial^2 w}{\partial x\,\partial y} \tag{4}$$

Assuming that both nanoplates bulk and surface are homogeneous and isotropic, the stress-strain relation of bulk material subjected to thermal effect are expressed by [37-40]:

$$\begin{Bmatrix} \sigma_{xx}^b \\ \sigma_{yy}^b \\ \sigma_{xy}^b \end{Bmatrix} = \begin{bmatrix} E/(1-v^2) & vE/(1-v^2) & 0 \\ vE/(1-v^2) & E/(1-v^2) & 0 \\ 0 & 0 & G \end{bmatrix} \begin{Bmatrix} \varepsilon_{xx} \\ \varepsilon_{yy} \\ \gamma_{xy} \end{Bmatrix} - \begin{Bmatrix} E\,\alpha\,\Delta T/(1-v) \\ E\,\alpha\,\Delta T/(1-v) \\ 0 \end{Bmatrix} \tag{5}$$

where E, v, G, α, and ΔT denote the elastic modulus, Poisson's ratio, shear modulus, thermal expansion coefficient, and uniform temperature change, respectively. b is the superscript for bulk properties and effects. The constitutive relations of the surface layers s^+ and s^-, as given by Gurtin and Murdoch [7], can be expressed as [10, 18, 33, 48]:

$$\sigma_{\alpha\beta}^{s\pm} = \tau^{s\pm}(\delta_{\alpha\beta}+u_{\alpha,\beta})+(\mu^{s\pm}-\tau^{s\pm})(u_{\alpha,\beta}+u_{\beta,\alpha})+(\lambda^{s\pm}+\tau^{s\pm})u_{\gamma,\gamma}\delta_{\alpha\beta} \;,\; \alpha,\beta,\gamma = x,y \quad (z = \pm\frac{h}{2})$$

$$\sigma_{\alpha z}^{s\pm} = \tau^{s\pm}u_{z,\alpha} \;, \qquad \alpha = x,y \tag{6}$$

where $\delta_{\alpha\beta}$ is the Kronecker delta and $\alpha = \beta = \gamma = x, y$. $\tau^{s\pm}$ are the residual surface tension components in Newtons per meter under unconstrained conditions, while $\lambda^{s\pm}$ and $\mu^{s\pm}$ are the surface Lame constants on the s^+ and s^- surfaces, respectively. If the top and bottom layers have the same material properties, the stress–strain relations become [10,18,33,48]:

$$\sigma_{xx}^{s\pm} = \tau^s + (2\mu^s + \lambda^s)\varepsilon_{xx} + (\tau^s + \lambda^s)\varepsilon_{yy} = \tau^s \mp \frac{h}{2}(2\mu^s + \lambda^s)\frac{\partial^2 w}{\partial x^2} \mp \frac{h}{2}(\tau^s + \lambda^s)\frac{\partial^2 w}{\partial y^2}$$

$$\sigma_{yy}^{s\pm} = \tau^s + (2\mu^s + \lambda^s)\varepsilon_{yy} + (\tau^s + \lambda^s)\varepsilon_{xx} = \tau^s \mp \frac{h}{2}(2\mu^s + \lambda^s)\frac{\partial^2 w}{\partial y^2} \mp \frac{h}{2}(\tau^s + \lambda^s)\frac{\partial^2 w}{\partial x^2} \tag{7}$$

$$\sigma_{xy}^{s\pm} = \frac{1}{2}(2\mu^s - \tau^s)\gamma_{xy} = \mp\frac{h}{2}(2\mu^s - \tau^s)\frac{\partial^2 w}{\partial x\,\partial y}$$

$$\sigma_{xz}^{s\pm} = \tau^s\frac{\partial w}{\partial x} \;,\; \sigma_{yz}^{s\pm} = \tau^s\frac{\partial w}{\partial y}$$

The resultant stresses are defined as [10, 18, 33, 48]:

$$M_{\alpha\beta} = \int_{-h/2}^{h/2} \sigma_{\alpha\beta}^{b} z \, dz + (\sigma_{\alpha\beta}^{s+} - \sigma_{\alpha\beta}^{s-})\frac{h}{2} \qquad \alpha, \beta = x, y$$

$$N_{\alpha\beta} = \int_{-h/2}^{h/2} \sigma_{\alpha\beta}^{b} \, dz + (\sigma_{\alpha\beta}^{s+} + \sigma_{\alpha\beta}^{s-}) \qquad \alpha, \beta = x, y$$

(8)

Using Eqs. (2, 4, 5, 7, 8), the stress resultant can be expressed in terms of the displacement components as [10,18,33,48]:

$$M_{xx} - g^{2}\nabla^{2}M_{xx} = -\left(D + \frac{h^{2}(2\mu^{s} + \lambda^{s})}{2}\right)\frac{\partial^{2}w}{\partial x^{2}} - \left(\nu D + \frac{h^{2}(\tau^{s} + \lambda^{s})}{2}\right)\frac{\partial^{2}w}{\partial y^{2}},$$

$$M_{yy} - g^{2}\nabla^{2}M_{yy} = -\left(D + \frac{h^{2}(2\mu^{s} + \lambda^{s})}{2}\right)\frac{\partial^{2}w}{\partial y^{2}} - \left(\nu D + \frac{h^{2}(\tau^{s} + \lambda^{s})}{2}\right)\frac{\partial^{2}w}{\partial x^{2}},$$

(9)

$$M_{xy} - g^{2}\nabla^{2}M_{xy} = -\left(D(1-\nu) + \frac{h^{2}(2\mu^{s} - \tau^{s})}{2}\right)\frac{\partial^{2}w}{\partial x \partial y}$$

where $D = Eh^{3}/12(1-\nu^{2})$ is the flexural rigidity of the nanoplate. The equations of motion, considering both the nonlocal effect and surface energy, can be derived using Hamilton's principle. The variation of strain energy of the nanoplate, δU_{i}, can be written as [48]:

$$\delta U_{i} = \frac{1}{2}\int_{V}(\sigma_{xx}\delta\varepsilon_{xx} + \sigma_{yy}\delta\varepsilon_{yy} + \sigma_{xy}\delta\gamma_{xy} + \sigma_{yz}\delta\gamma_{yz} + \sigma_{xz}\delta\gamma_{xz})dA \, dz$$

$$= \frac{1}{2}\int_{A}\left\{-M_{xx}\frac{\partial^{2}\delta w}{\partial x^{2}} - M_{yy}\frac{\partial^{2}\delta w}{\partial y^{2}} - 2M_{xy}\frac{\partial^{2}\delta w}{\partial x \partial y} + 2\tau^{s}\left(\frac{\partial w}{\partial x}\frac{\partial \delta w}{\partial x} + \frac{\partial w}{\partial y}\frac{\partial \delta w}{\partial y}\right)\right\}dA$$

(10)

The variation of potential energy of the conservative loads, δU_{e}, can be written as [37-40, 48]:

$$\delta U_{e} = \frac{1}{2}\int_{A}\left\{(N_{xx} + N_{xx}^{th})\left(\frac{\partial w}{\partial x}\frac{\partial \delta w}{\partial x}\right) + 2(N_{xy} + N_{xy}^{th})\left(\frac{\partial w}{\partial x}\frac{\partial \delta w}{\partial y}\right) + (N_{yy} + N_{yy}^{th})\left(\frac{\partial w}{\partial y}\frac{\partial \delta w}{\partial y}\right)\right\}dx \, dy$$

$$+ \int_{S}\left\{-q\,\delta w + k_{0W}w\,\delta w + k_{0S}\left(\frac{\partial w}{\partial x}\frac{\partial \delta w}{\partial x} + \frac{\partial w}{\partial y}\frac{\partial \delta w}{\partial y}\right)\right\}dx \, dy$$

(11)

where $q, N_{\alpha\beta}$, and $N^{th}_{\alpha\beta}$ are the transverse and in-plane loads. k_{0W} and k_{0S} are the Winkler and shear moduli of the foundation, respectively. The thermal force, $N^{th}_{\alpha\beta}$, can be expressed as [37-40]:

$$N_{xx}^{th} = N_{yy}^{th} = -\frac{E h \alpha}{(1-\nu)}\Delta T, \qquad N_{xy}^{th} = 0$$

(12)

To derive the governing equation of equilibrium, principle of virtual work is used. The principle can be stated in analytical form as [48]:

$$\int_{0}^{t}(\delta U_{i} + \delta U_{e})\,dt = 0$$

(13)

Substituting Eqs. (10, 11, 13), the governing equations can be obtained, as follows [10, 18, 33, 37-40, 48]:

$$\frac{\partial^2 M_{xx}}{\partial x^2} + 2\frac{\partial^2 M_{xy}}{\partial x\,\partial y} + \frac{\partial^2 M_{yy}}{\partial y^2} + \left((N_{xx} + N_{xx}^{th})\frac{\partial^2 w}{\partial x^2} + 2(N_{xy} + N_{xy}^{th})\frac{\partial^2 w}{\partial x\,\partial y} + (N_{yy} + N_{yy}^{th})\frac{\partial^2 w}{\partial y^2} \right)$$
$$+ 2\tau^s\nabla^2(w) + q - k_{0W}w + k_{0S}\nabla^2(w) = 0 \tag{14}$$

Fig. 1 shows the geometry of rectangular nanoplate and the loading conditions. In the present study, it is assumed that the nanoplate is free from any transverse loadings ($q = 0$). Using Eqs. (9,12), the governing Eq. (14) can be expressed in terms of displacement components, as follows [10,18,33,37-40,48]:

$$(D + \frac{h^2 E^s}{2})(\nabla^4 w) - 2\tau^s(1 - g^2\nabla^2)(\nabla^2 w) - \left(-\frac{E\,h\,\alpha}{(1-\nu)}\Delta T \right)(1 - g^2\nabla^2)(\nabla^2 w)$$
$$-(1 - g^2\nabla^2)\left\{ N_{xx}\frac{\partial^2 w}{\partial x^2} + 2N_{xy}\frac{\partial^2 w}{\partial x\,\partial y} + N_{yy}\frac{\partial^2 w}{\partial y^2} \right\} + k_{0W}(1 - g^2\nabla^2)(w) - k_{0G}(1 - g^2\nabla^2)(\nabla^2 w) = 0 \tag{15}$$

where $E^s = 2\mu^s + \lambda^s$, $\nabla^4 = \left(\partial^4 w / \partial x^4 \right) + \left(2\partial^4 w / \partial x^2 \partial y^2 \right) + \left(\partial^4 w / \partial y^4 \right)$.
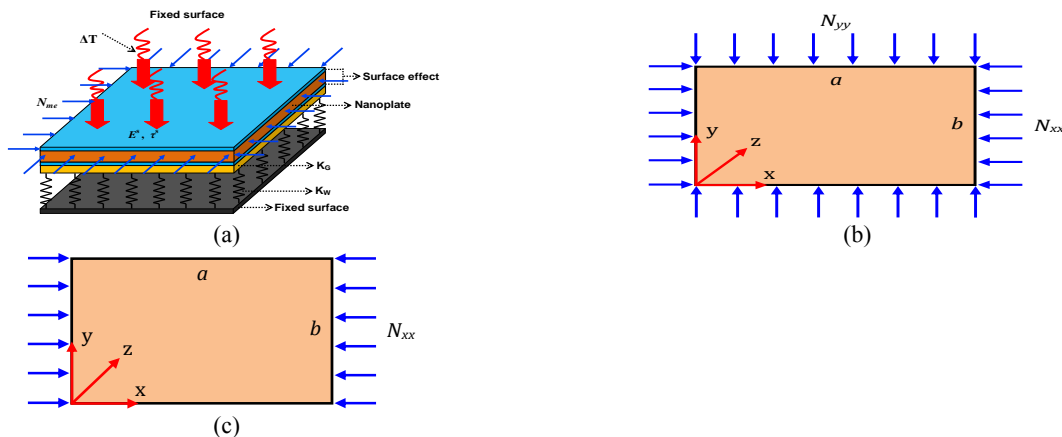
Fig .1
(a) The geometry of rectangular nanoplate with surface layers and thermal loading, (b) Biaxial loading, (c) Uniaxial loading.

3 SOLUTION PROCEDURE
3.1 Navier's method

Based on the Navier's method, the exact solution for buckling of rectangular nanoplates, regarding simply-supported boundary condition is expressed by:

$$w = \sum_{m=1}^{\infty}\sum_{n=1}^{\infty} w_{mn}\sin(\gamma x)\sin(\lambda y) \tag{16}$$

where $\gamma = m\pi/a$, and $\lambda = n\pi/b$. m and n are half-wave number along x and y direction. Substituting Eq.(16) into Eq.(15), the critical buckling load, N_{cr}, is obtained:

For biaxial buckling $N_{xx} = N_{yy} = N_{cr}, N_{xy} = 0$. Therefore, the critical buckling load is expressed by:

$$N_{cr} = \frac{1}{(\eta + g^2\eta^2)} \times \left[\begin{array}{l} \left(D + \dfrac{h^2 E^s}{2} \right)\eta^2 + 2\tau^2\left(\eta + g^2\eta^2 \right) \\ + \left\{ \dfrac{-E\,h\,\alpha\,\Delta T}{(1-\nu)} \right\}(\eta + g^2\eta^2) + k_{0W}\left(1 + g^2\eta \right) + k_{0S}\left(\eta + g^2\eta^2 \right) \end{array} \right] \tag{17}$$

For uniaxial buckling $N_{xx} = N_{cr}, N_{yy} = N_{xy} = 0$. Therefore, the critical buckling load is expressed by:

$$N_{cr} = \frac{1}{\left(\gamma^2 + g^2\left(\gamma^4 + \gamma^2\lambda^2\right)\right)} \times \left[\begin{array}{l} \left(D + \dfrac{h^2 E^s}{2}\right)\eta^2 + 2\tau^2\left(\eta + g^2\eta^2\right) \\[2mm] + \left\{\dfrac{-E\,h\alpha\,\Delta T}{(1-v)}\right\}\left(\eta + g^2\eta^2\right) + k_{0W}\left(1 + g^2\eta\right) + k_{0S}\left(\eta + g^2\eta^2\right) \end{array} \right] \tag{18}$$

where $\eta = \gamma^2 + \lambda^2$.

3.2 Finite difference method

The finite difference method is a simple method for solving differential equations. In recent years, Karamooz Ravari et al. [49,50] studied nonlocal effect on the buckling of rectangular and circular nanoplates using FDM. The FDM substitutes the nanoplate differential equation and the expressions which define the boundary conditions with equal differences equations. Therefore, the solution of the bending problem is reduced to the simultaneous solution of a set of algebraic equations written for every nodal point within the nanoplate. Fig. 2 shows a rectangular nanoplate and the grid points which could be used in the finite difference method. By using this method, Eq. (19) can be used to estimate the derivative of the transverse displacement, *w*, for the *i,j*-th point as a function of its neighboring points.

$$\frac{dw}{dx} = \frac{1}{2r_x}\left(w_{(i+1,j)} - w_{(i-1,j)}\right) \tag{19}$$

Here r_x and r_y are the distance between two grid points in the *x* and *y* directions, respectively. Substituting Eq. (19) into Eq. (15) and developing a computer code in MATLAB the governing equation are solved.

$$\begin{aligned}
&\left(D + \frac{h^2 E^s}{2} + 2\tau^s g^2 - \frac{E\,h\alpha}{(1-v)}\Delta T\,g^2 + k_{0G}\,g^2\right)\left\{\frac{1}{r_x^4}\left(w_{(i+2,j)} - 4w_{(i+1,j)} + 6w_{(i,j)}\right.\right. \\
&\left.-4w_{(i-1,j)} + w_{(i-2,j)}\right) + \frac{1}{r_y^4}\left(w_{(i,j+2)} - 4w_{(i,j+1)} + 6w_{(i,j)} - 4w_{(i,j-1)} + w_{(i,j-2)}\right) \\
&+ \frac{2}{r_x^2 r_y^2}\left(w_{(i+1,j+1)} + w_{(i-1,j+1)} + w_{(i-1,j-1)} + w_{(i+1,j-1)} + 4w_{(i,j)}\right) \\
&\left.-\frac{4}{r_x^2 r_y^2}\left(w_{(i+1,j)} + w_{(i,j+1)} + w_{(i-1,j)} + w_{(i,j-1)}\right)\right\} \\
&+ \left(-2\tau^s + \frac{E\,h\alpha}{(1-v)}\Delta T - k_{0G} - k_{0W}\,g^2\right)\left\{\frac{1}{r_x^2}\left(w_{(i+1,j)} - 2w_{(i,j)} + w_{(i-1,j)}\right)\right. \\
&\left.+ \frac{1}{r_y^2}\left(w_{(i,j+1)} - 2w_{(i,j)} + w_{(i,j-1)}\right)\right\} + k_{0W}\,w_{(i,j)} \\
&+ N_{xx}\left\{\frac{1}{r_x^2}\left(w_{(i+1,j)} - 2w_{(i,j)} + w_{(i-1,j)}\right) + \frac{1}{r_x^2 r_y^2}\left(w_{(i+1,j+1)} + w_{(i-1,j+1)} + w_{(i-1,j-1)}\right.\right. \\
&\left.\left.+ w_{(i+1,j-1)} + 4w_{(i,j)}\right) - \frac{2}{r_x^2 r_y^2}\left(w_{(i+1,j)} + w_{(i,j+1)} + w_{(i-1,j)} + w_{(i,j-1)}\right)\right\} \\
&+ N_{yy}\left\{\frac{1}{r_y^2}\left(w_{(i,j+1)} - 2w_{(i,j)} + w_{(i,j-1)}\right) + \frac{1}{r_x^2 r_y^2}\left(w_{(i+1,j+1)} + w_{(i-1,j+1)} + w_{(i-1,j-1)}\right.\right. \\
&\left.\left.+ w_{(i+1,j-1)} + 4w_{(i,j)}\right) - \frac{2}{r_x^2 r_y^2}\left(w_{(i+1,j)} + w_{(i,j+1)} + w_{(i-1,j)} + w_{(i,j-1)}\right)\right\} = 0
\end{aligned} \tag{20}$$
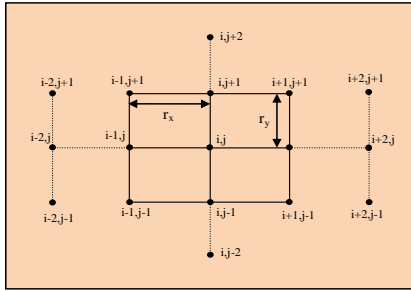
Fig .2
The rectangular nanoplate and finite difference grid points.

3.3 Boundary conditions

In this paper, the simply-supported and clamped boundary conditions are investigated. Therefore, in this subsection these boundary conditions are introduced.

3.3.1 Simply-supported boundary conditions

The simply-supported boundary conditions at all edges of nanoplate can be written as:

$$\frac{\partial^2 w}{\partial x^2} = 0 \qquad \frac{\partial^2 w}{\partial y^2} = 0 \qquad w = 0 \tag{21}$$

These conditions lead to the following expressions:

$$w_{(i,j)} = -w_{(i,j+2)}, \quad w_{(i,j)} = -w_{(i,j-2)}, \quad w_{(i,j+3)} = -w_{(i,j-1)}, \quad w_{(i,j-3)} = -w_{(i,j+1)}$$

$$w_{(i,j)} = -w_{(i-2,j)}, \quad w_{(i,j)} = -w_{(i+2,j)}, \quad w_{(i-3,j)} = -w_{(i+1,j)}, \quad w_{(i+3,j)} = -w_{(i-1,j)} \tag{22}$$

$$w_{(i,j\pm1)} = w_{(i+1,j\pm1)} = w_{(i-1,j\pm1)} = w_{(i\pm1,j)} = 0$$

3.3.2 Clamped boundary conditions

The clamped boundary conditions could be expressed as follows:

$$\frac{\partial w}{\partial x} = 0 \qquad \frac{\partial w}{\partial y} = 0 \qquad w = 0 \tag{23}$$

These conditions lead to the following expressions:

$$w_{(i,j)} = w_{(i,j+2)}, \quad w_{(i,j)} = w_{(i,j-2)}, \quad w_{(i,j+3)} = w_{(i,j-1)}, \quad w_{(i,j-3)} = w_{(i,j+1)}$$

$$w_{(i,j)} = w_{(i-2,j)}, \quad w_{(i,j)} = w_{(i+2,j)}, \quad w_{(i-3,j)} = w_{(i+1,j)}, \quad w_{(i+3,j)} = w_{(i-1,j)} \tag{24}$$

$$w_{(i,j\pm1)} = w_{(i+1,j\pm1)} = w_{(i-1,j\pm1)} = w_{(i\pm1,j)} = 0$$

4   RESULTS AND DISCUSSION

In this section, it is attempted to demonstrate the surface energy and thermal effects on the buckling of rectangular nanoplate based on nonlocal elasticity theory. The validity of the suggested model is checked by comparing the results with those given in the literature. Moreover, the effects of important parameters including, the Winkler and

shear elastic moduli, the boundary conditions, in-plane biaxial and uniaxial loads, and width-to-length aspect ratio, on the surface stress effects are also studied. The isotropic material properties are taken as that of silver nanoplate. The material properties of the nanoplate are: $E = 76 GPa$, $v = 0.3$. The surface elastic modulus and surface residual stress are $E^s = 1.22 N/m$, and $\tau^s = 0.89 N/m$, respectively [26]. Moreover, $K_W = k_{0W} a^4 / D$ and $K_G = k_{0G} a^2 / D$ are non-dimensional Winkler and shear moduli of the elastic foundation, respectively. For all examples, supposed $h = 1nm$, $a = 10nm$, $g = 1nm$, $\Delta T = 50^\circ K$, $K_W = 100$, $K_G = 10$, $\mu^s = 0.47 N/m$, and $\lambda^s = 0.28 N/m$, unless noted otherwise. The coefficient of thermal expansion is $\alpha = 1.9 \times 10^{-6} K^{-1}$ [51]. For the sake of brevity, a six-letter symbol is used to represent the boundary conditions for the following four edges of the rectangular nanoplate, as shown in Fig. 3.
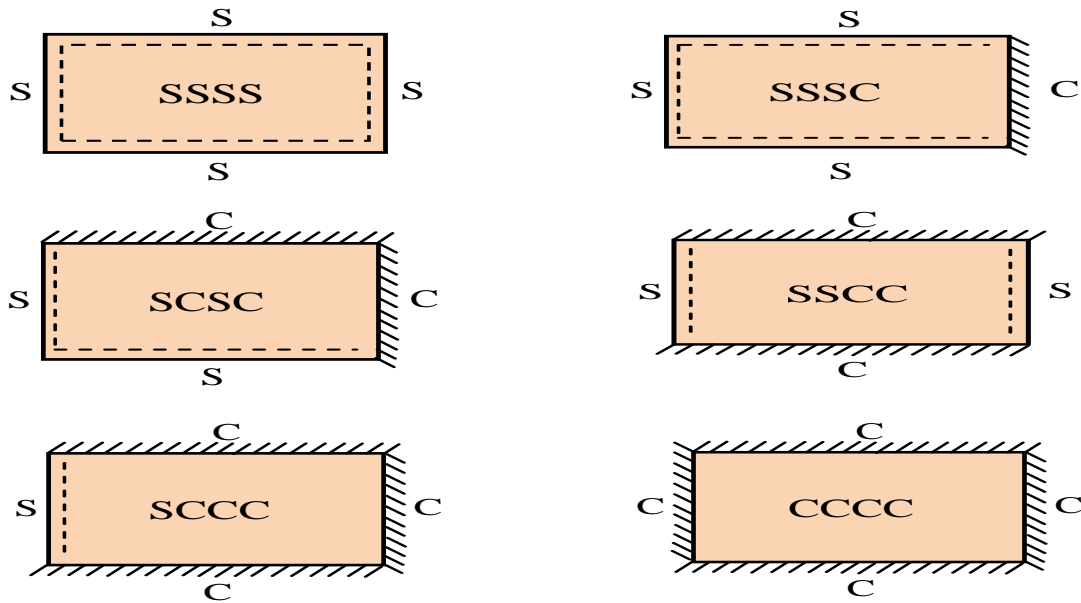

Fig .3
Combinations of boundary conditions, S: simply-supported, C: clamped.

For analysis of numerical results, the buckling ratio is defined as follows:

$$\text{buckling ratio=} \frac{\textit{Critical buckling load with surface stress effects } (N_s)}{\textit{Critical buckling load without surface stress effects } (N)} \qquad (25)$$

Finite difference method results are sensitive to lower grid points, a convergence test is performed to determine the minimum number of grid points required to obtain stable and accurate results for Eq. (20). In Fig. 4, non-dimensional buckling load ($N_{cr} a^2 / D$) of square nanoplate is plotted versus the number of grid points for various boundary conditions. Both of non-dimensional biaxial and uniaxial buckling loads are studied in Fig. 4. According to Fig. 4, the present solution is converging. From this figure, it is clearly seen that fourteen number of grid points (N=M=14) are sufficient to obtain the accurate solutions for the buckling analyses. It should be noted that, M and N are the number of grid points in the x and y directions, respectively.
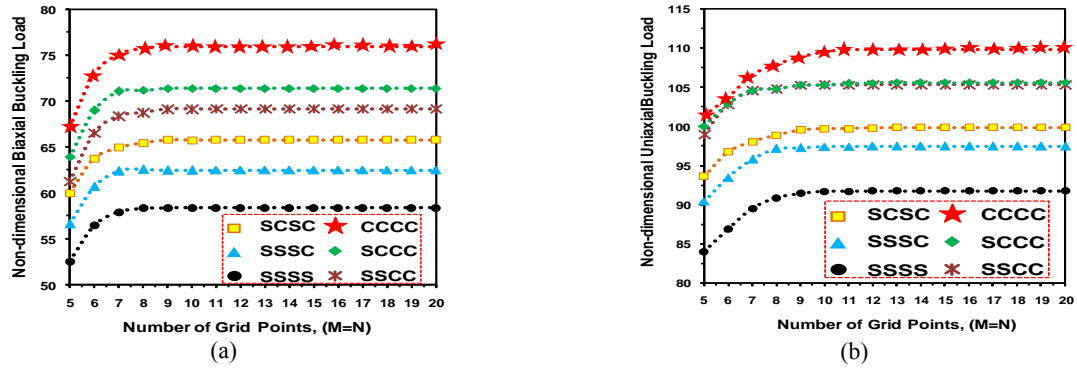
Fig .4
Convergence study and minimum number of grid points required for obtaining accurate results for non-dimensional buckling load by finite difference method with various boundary conditions, (a) Biaxial buckling, (b) Uniaxial buckling.

Table 1. indicates the non-dimensional buckling load ($N_{cr}a^2/D$) of simply-supported square silver nanoplate versus nonlocal parameter for various length-to-thickness ratios, considering the surface energy effects but without considering the elastic medium and uniform temperature change. The results in [26] are based on an exact analytical solution. In the paper presented by Wang and Wang [26], the nonlocal effect is considered only for nanoplate bulk , while the present article by these authors, the nonlocal effect is considered for both nanoplate bulk and surface. This is reason of the difference between results presented by Wang and Wang and results presented by these authors. From this table, it is observed that the present results would be in good agreement with those of others reported in the literature [26] and also Navier's solutions.

Table 1
Comparison of non-dimensional buckling load of square nanoplates with all edges simply-supported ($a=10nm, E^s=1.22N/m$, $\tau^s=0.89N/m, \Delta T=0K, K_w=K_G=0$).

$g^2\ nm^2$	References	Biaxial buckling			Uniaxial buckling		
		$a/h=2$	5	10	$a/h=2$	5	10
0	[26]	20.290	23.801	47.045	40.580	47.602	94.090
	FDM	20.290	23.801	47.045	40.580	47.602	94.090
	Navier's solutions	20.290	23.801	47.045	40.580	47.602	94.090
1	[26]	17.0358	20.5472	43.7910	34.0716	41.0944	78.6791
	FDM	16.979	20.405	43.506	33.957	40.809	76.893
	Navier's solutions	16.979	20.405	43.506	33.957	40.809	76.893
2	[26]	14.7028	18.2142	41.4580	29.4056	36.4284	68.4212
	FDM	14.605	40.809	40.968	29.210	35.939	65.736
	Navier's solutions	14.605	40.809	40.968	29.210	35.939	65.736

Figs. 5(a) and 5(b) illustrate the influence of nanoplate aspect ratios, b/a, on the biaxial and uniaxial buckling ratios of rectangular nanoplate for different boundary conditions, respectively. It can be seen that by increasing the plate aspect ratio to $b/a=1.5$, the surface stress effects on the biaxial and uniaxial buckling ratios would increase drastically, while for aspect ratio larger than 1.5, $b/a \succ 1.5$, the surface energy on the buckling has no significant effects. Moreover, for higher values of aspect ratios, the surface energy effects are more dependent on the boundary conditions. Since, by incrementing the size of the nanoplate, the bending stiffness would reduce; accordingly, the strain energy of the bulk material would decrease, while the surface free energy-to-bulk energy ratio advances.

Figs. 6(a) and 6(b) demonstrate the effects of thickness, *h*, on the biaxial and uniaxial buckling ratios of square nanoplate for various boundary conditions. It is observed that by increasing the thickness of nanoplate, the biaxial and uniaxial buckling ratios would decrease seriously; therefore, the surface elasticity effects would also reduce drastically. Since by advancing the nanoplate thickness, the surface-to-volume ratio diminish; thus, the surface free energy-to-bulk energy ratio decreases. In addition, for higher degree of thickness, the surface stress effects are not dependent on the boundary conditions.
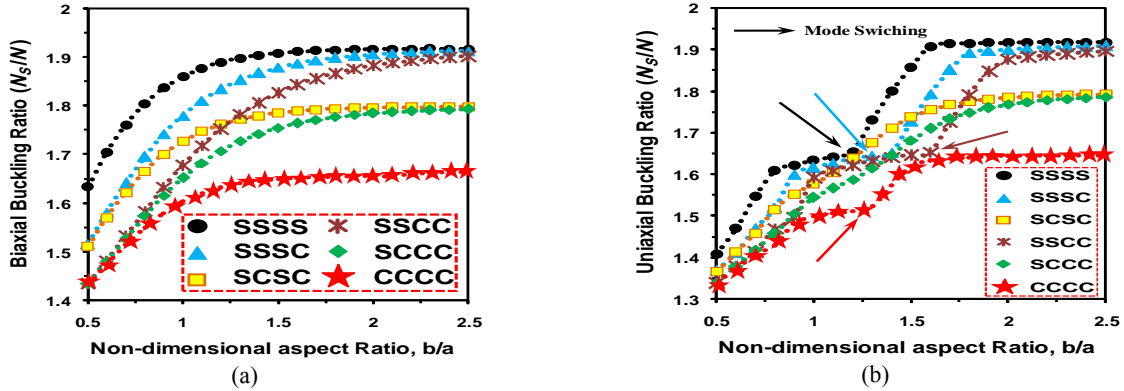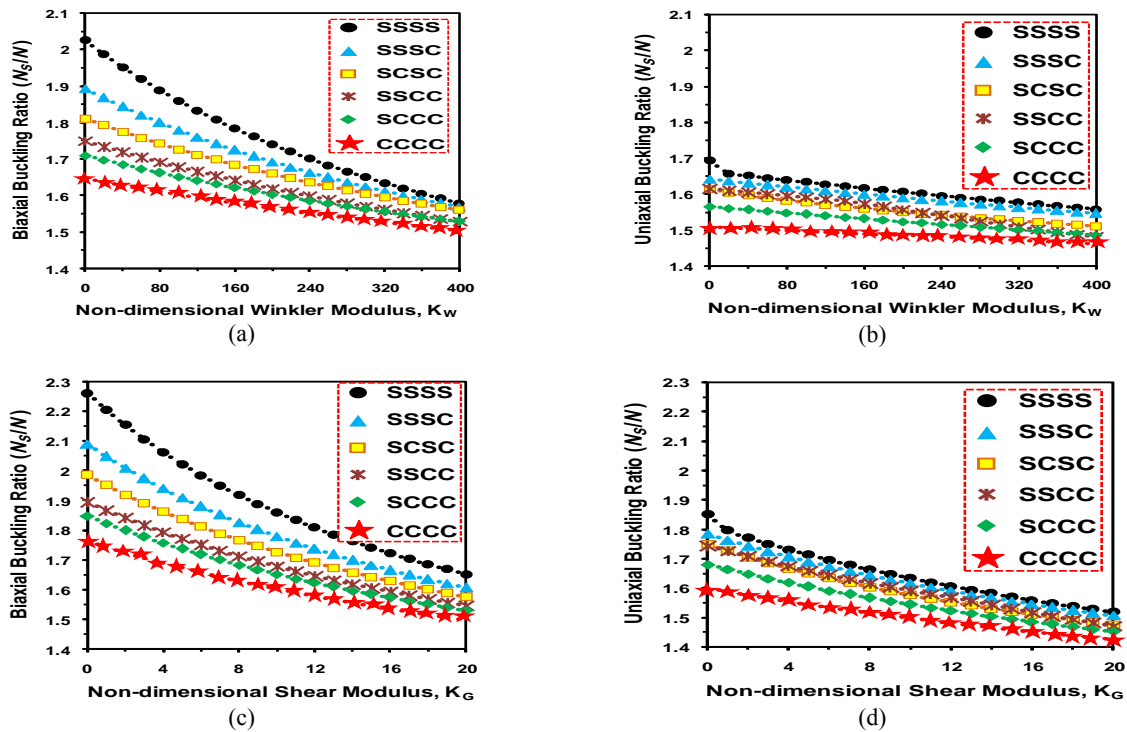
Fig .5
Buckling ratio of rectangular nanoplate versus aspect ratio, b/a, for various boundary conditions, (a) Biaxial buckling, (b) Uniaxial buckling.
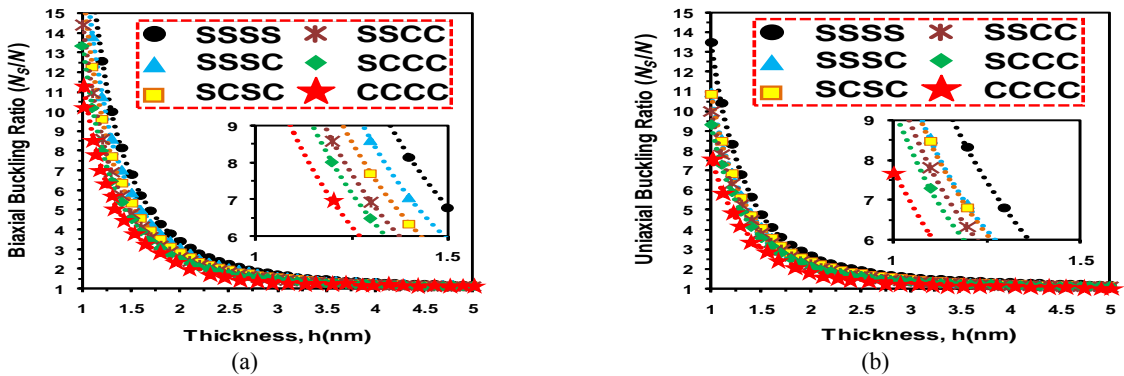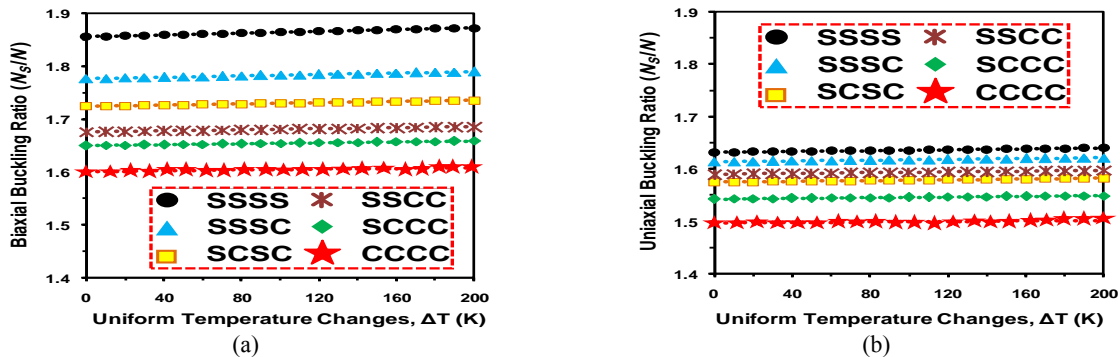

Fig .6
Buckling ratio of square nanoplate versus thickness, *h*, for various boundary conditions, (*a*=50 *nm*), (a) Biaxial buckling, (b) Uniaxial buckling.

Figs. 7(a, b) and 7(c, d) show the effects of Winkler and shear moduli on the buckling ratio of square nanoplates for different boundary conditions, respectively. For Fig. 7(a, b), the non-dimensional shear modulus is $K_G = 10$ and for Fig. 7(c, d), the non-dimensional Winkler modulus is $K_W = 100$. It could be seen that by improving the modulus of elastic medium, the biaxial and uniaxial buckling ratios would decrease. Therefore, the surface stress effects could also decrease. In the same way, it is observed that the effects of the boundary conditions would also decrease. In addition, as the boundary conditions become more rigid, the effects of elastic medium would diminish more. Moreover, the effects of Winkler and shear moduli on the biaxial buckling are more noticeable than that of uniaxial buckling. It is clear that an elastic medium could have a stiffening effect on a structural plate. By continuous rise of the elasticity of a medium, the stiffening property of surface energy effect cannot show itself for higher values of medium elasticity. This comment could be repeated for boundary conditions of different type, i.e., the effect of changing boundary conditions cannot be observed clearly for severe values of medium stiffness. On the contrary, by advancing the stiffening property of the in-plane loading (from biaxial toward uniaxial), the stiffening property of elastic medium could manifest itself less. Since, for biaxial buckling problems, the in-plane compressive loading is applied from all four sides of the nanoplate, while for uniaxial buckling problem, this loading is applied from only two opposite sides. Therefore, the plate stiffness should be the highest for uniaxial buckling case, and the lowest for biaxial buckling case.

Figs. 8(a) and 8(b) indicate the effects of uniform temperature changes on the biaxial and uniaxial buckling ratios of square nanoplates for different boundary conditions, respectively. It could be found that by augmenting the uniform temperature change, the biaxial and uniaxial buckling ratios would increase. Therefore, by increasing the temperature change, the value of surface energy effect would rise.

Fig .7
Buckling ratio of square nanoplates versus elastic moduli for various boundary conditions, (a) Winkler modulus and biaxial buckling, (b) Winkler modulus and uniaxial buckling, (c) Shear modulus and biaxial buckling, (d) Shear modulus and *c* buckling.
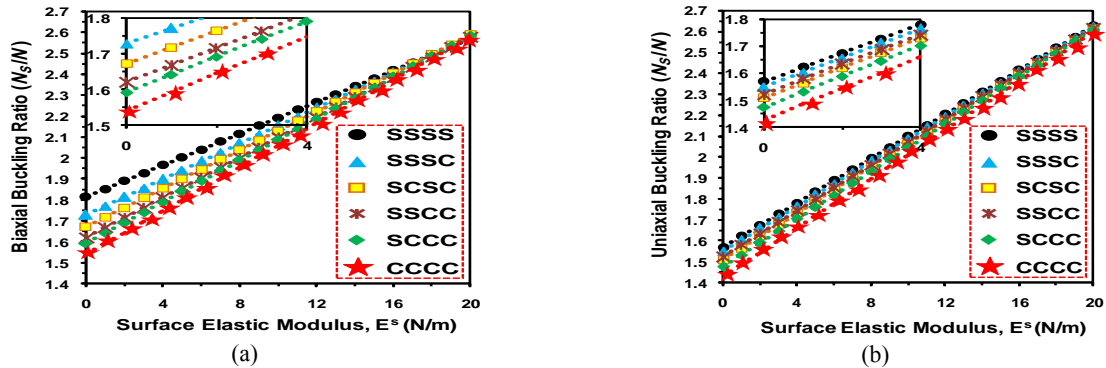

Fig .8
Buckling ratio of square nanoplates versus uniform temperature changes for various boundary conditions, (a) Biaxial buckling, (b) Uniaxial buckling.

Figs. 9(a) and 9(b) show the effects of surface elastic modulus, E^s, on the biaxial and uniaxial buckling ratios of square nanoplate for various boundary conditions. For Fig. 9, the surface residual stress is $\tau^s = 0.89 N / m$. It can be seen that by increasing the surface elastic modulus, the biaxial and uniaxial buckling ratios would increase drastically. Therefore, by increasing the surface elastic modulus, the value of surface effect would improve seriously. Moreover, for higher degree of surface elastic modulus, the surface stress effects are not dependent on the boundary conditions. In addition, it is observed that, the effects of surface elastic modulus on the uniaxial buckling are more noticeable than that of biaxial buckling.
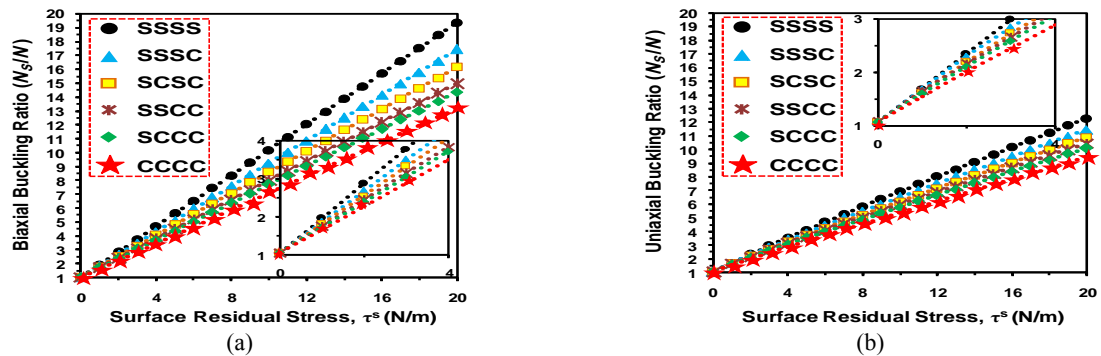
Figs. 10(a) and 10(b) demonstrate the effects of surface residual stress, τ^s, on the biaxial and uniaxial buckling ratios of square nanoplate for various boundary conditions. For Fig.10, the surface elastic modulus is $E^s = 1.22 N/m$. It can be found that by augmenting the surface residual stress, the biaxial and uniaxial buckling ratios would advance drastically; therefore, the degree of surface energy effect would increase seriously. In addition,

for higher value of surface residual stress, the surface stress effects are dependent on the boundary conditions. This situation is the opposite of result surface elastic modulus, E^s. Moreover, it is observed that, the effects of surface residual stress on the biaxial buckling are more noticeable than that of uniaxial buckling. This result is the opposite of result surface elastic modulus, E^s. On the other hand, by comparing Figs. 9 and 10 it is found that the surface residual stress on the biaxial and uniaxial buckling are more important than that of surface elastic modulus.

Since, the surface energy effects are total of surface elastic modulus and surface residual stress effects and surface residual stress on the biaxial and uniaxial buckling are more noticeable than that of surface elastic modulus. Therefore, the surface elasticity effects on the biaxial buckling are more pronounced than that of uniaxial buckling.

(a)   (b)

Fig .9
Buckling ratio of square nanoplates versus surface elastic modulus for various boundary conditions, (a) Biaxial buckling, (b) Uniaxial buckling.

(a)   (b)

Fig .10
Buckling ratio of square nanoplates versus surface residual stress for various boundary conditions, (a) Biaxial buckling, (b) Uniaxial buckling.

5   CONCLUSIONS

In this article, surface stress and nonlocal effects on the biaxial and uniaxial buckling of rectangular silver nanoplates resting on elastic foundations were studied using finite difference method (FDM). The uniform temperature change was used to investigate thermal effect. The small scale and surface energy effects were taken into account using the Eringen's nonlocal elasticity and Gurtin-Murdoch's theory, respectively. Using the principle of virtual work, the governing equations considering small scale for both nanoplate bulk and surface were derived. The finite difference method, uniaxial buckling, nonlocal effect for both nanoplate bulk and surface, silver material properties, and below-mentioned results were the novelty of this investigation. According to the selected numerical results, it was observed that the surface energy effects and temperature environments on the biaxial and uniaxial buckling were remarkable such that they cannot be ignored. Results show that the finite difference method could be used to solve a variety of problems with different types of boundary condition with little computational effort. It was observed that with increasing the nonoplate aspect ratio to $b/a = 1.5$, the surface stress effects would increase drastically, while for aspect ratio larger than 1.5, $b/a \succ 1.5$, the surface energy on the biaxial and uniaxial buckling

had no significant effects. Moreover, it could be seen that by improving the thickness of nanoplate, *h*, the degree of surface stress effects diminished seriously. Furthermore, it was found that the influences of surface elastic modulus on the uniaxial buckling were more noticeable than that of biaxial buckling, but the influences of surface residual stress on the biaxial buckling were more noticeable than that of uniaxial buckling. In addition, it was observed that the effects of Winkler, shear moduli, and surface energy on the biaxial buckling were more pronounced than that of uniaxial buckling.

REFERENCES

[1]   Sakhaee-Pour A., Ahmadian M. T., Vafai A., 2008, Applications of single-layered graphene sheets as mass sensors and atomistic dust detectors, *Solid State Communications* **145**:168-172.

[2]   Ball P., 2001, Roll up for the revolution, *Nature* **414**:142-144.

[3]   Baughman R. H., Zakhidov A. A., DeHeer W. A., 2002, Carbon nanotubes–the route toward applications, *Science* **297**: 787-792.

[4]   Li C., Chou T. W., 2003, A structural mechanics approach for the analysis of carbon nanotubes, *International Journal of Solids and Structures* **40**: 2487-2499.

[5]   Govindjee S., Sackman J. L., 1999, On the use of continuum mechanics to estimate the properties of nanotubes, *Solid State Communications* **110**: 227-230.

[6]   He X. Q., Kitipornchai S., Liew K. M., 2005, Buckling analysis of multi-walled carbon nanotubes: a continuum model accounting for van der Waals interaction, *Journal of Mechanics and Physics of solids* **53**: 303-326.

[7]   Gurtin M. E., Murdoch A. I., 1975, A continuum theory of elastic material surfaces, *Archive for Rational Mechanics and Analysis* **57**: 291-323.

[8]   Gurtin M. E, Murdoch A. I., 1978, Surface stress in solids*, International Journal of Solids and Structures* **14**: 431-440.

[9]   Assadi A., Farshi B., Alinia-Ziazi A., 2010, Size dependent dynamic analysis of nanoplates, *Journal of Applied Physics* **107**: 124310.

[10]   Assadi A., 2013, Size dependent forced vibration of nanoplates with consideration of surface effects, *Applied Mathematical Modelling* **37**: 3575-3588.

[11]   Assadi A., Farshi B., 2010, Vibration characteristics of circular nanoplates, *Journal of Applied Physics* **108**: 074312.

[12]   Assadi A., Farshi B., 2011, Size dependent stability analysis of circular ultrathin films in elastic medium with consideration of surface energies, *Physica E* **43**: 1111-1117.

[13]   Gheshlaghi B., Hasheminejad S. M., 2011, Surface effects on nonlinear free vibration of nanobeams, *Composites Part B: Engineering* **42**: 934-937.

[14]   Nazemnezhad R., Salimi M., Hosseini Hashemi S. h., Asgharifard Sharabiani P., 2012, An analytical study on the nonlinear free vibration of nanoscale beams incorporating surface density effects, *Composites Part B: Engineering* **43**: 2893-2897.

[15]   Hosseini-Hashemi S., Nazemnezhad R., 2013, An analytical study on the nonlinear free vibration of functionally graded nanobeams incorporating surface effects, *Composites Part B: Engineering* **52**: 199-206.

[16]   Asgharifard Sharabiani P., Haeri Yazdi M. R., 2013, Nonlinear free vibrations of functionally graded nanobeams with surface effects, *Composites Part B: Engineering* **45**: 581-586.

[17]   Ansari R., Sahmani S., 2011, Bending behavior and buckling of nanobeams including surface stress effects corresponding to different beam theories, *International Journal of Engineering Science* **49**: 1244-1255.

[18]   Karimi M., Shokrani M.H., Shahidi A.R., 2015, Size-dependent free vibration analysis of rectangular nanoplates with the consideration of surface effects using finite difference method, *Journal of Applied and Computational Mechanics* **1**: 122-133.

[19]   Challamel N., Elishakoff I., 2012, Surface stress effects may induce softening: Euler–Bernoulli and Timoshenko buckling solutions, *Physica E* **44**: 1862-1867.

[20]   Park H.S., 2012, Surface stress effects on the critical buckling strains of silicon nanowires, *Computational Materials Science* **51**: 396-401.

[21]   Ansari R., Shahabodini A., Shojaei M. F., Mohammadi V., Gholami R., 2014, On the bending and buckling behaviors of Mindlin nanoplates considering surface energies, *Physica E* **57**: 126-137.

[22]   Ansari R., Mohammadi V., Faghih Shojaei M., Gholami R., Sahmani S., 2014, On the forced vibration analysis of Timoshenko nanobeams based on the surface stress elasticity theory, *Composites Part B: Engineering* **60**: 158-166.

[23]   Mouloodi S., Khojasteh J., Salehi M., Mohebbi S., 2014, Size dependent free vibration analysis of Multicrystalline nanoplates by considering surface effects as well as interface region, *International Journal of Mechanical Sciences* **85**: 160-167.

[24]   Mouloodi S., Mohebbi S., Khojasteh J., Salehi M., 2014, Size-dependent static characteristics of multicrystalline nanoplates by considering surface effects, *International Journal of Mechanical Sciences* **79**: 162-167.

[25]   Wang K. F., Wang B. L., 2013, A finite element model for the bending and vibration of nanoscale plates with surface effect, *Finite Elements in Analysis and Design* **74**: 22-29.

[26] Wang K.F., Wang B.L., 2011, Combining effects of surface energy and non-local elasticity on the buckling of nanoplates, *Micro and Nano Letters* **6**: 941-943.

[27] Wang K.F., Wang B.L., 2011, Vibration of nanoscale plates with surface energy via nonlocal elasticity, *Physica E* **44**: 448-453.

[28] Farajpour A., Dehghany M., Shahidi A. R., 2013, Surface and nonlocal effects on the axisymmetric buckling of circular graphene sheets in thermal environment, *Composites Part B: Engineering* **50**: 333-343.

[29] Asemi S. R., Farajpour A., 2014, Decoupling the nonlocal elasticity equations for thermo-mechanical vibration of circular graphene sheets including surface effects, *Physica E* **60**: 80-90.

[30] Juntarasaid C., Pulngern T., Chucheepsakul S., 2012, Bending and buckling of nanowires including the effects of surface stress and nonlocal elasticity, *Physica E* **46**: 68-76.

[31] Mahmoud F.F., Eltaher M.A., Alshorbagy A.E., Meletis E.I., 2012, Static analysis of nanobeams including surface effects by nonlocal finite element, *Journal of Mechanical Science and Technology* **26**: 3555-3563.

[32] Eltaher M.A., Mahmoud F.F., Assie A.E., Meletis E.I., 2013, Coupling effects of nonlocal and surface energy on vibration analysis of nanobeams, *Applied Mathematics and Computation* **224**:760-774.

[33] Karimi M., Haddad H.A., Shahidi A.R., 2015, Combining surface effects and non-local two variable refined plate theories on the shear/biaxial buckling and vibration of silver nanoplates, *Micro and Nano Letters* **10**: 276-281.

[34] Hosseini–Hashemi S. h., Fakher M., Nazemnezhad R., 2013, Surface effects on free vibration analysis of nanobeams using nonlocal elasticity: a comparison between Euler-Bernoulli and Timoshenko, *Journal of Solid Mechanics* **5**: 290-304.

[35] Ghorbanpour Arani A., Kolahchi R., Hashemian M.,2014, Nonlocal surface piezoelasticity theory for dynamic stability of double-walled boron nitride nanotube conveying viscose fluid based on different theories, *Proceedings of the Institution of Mechanical Engineers, Part C: Journal of Mechanical Engineering Science* **203**:228-245.

[36] Ghorbanpour Arani A., Fereidoon A., Kolahchi R., 2014, Nonlinear surface and nonlocal piezoelasticity theories for vibration of embedded single-layer boron nitride sheet using harmonic differential quadrature and differential cubature methods, *Journal of Intelligent Material Systems and Structures* **26**:1150-1163.

[37] Mohammadi M., Moradi A., Ghayour M., Farajpour A., 2014, Exact solution for thermo-mechanical vibration of orthotropic mono-layer graphene sheet embedded in an elastic medium, *Latin American Journal of Solids and Structures* **11**: 437-458.

[38] Mohammadi M., Farajpour A., Goodarzi M., Dinari F., 2014, Thermo-mechanical vibration analysis of annular and circular graphene sheet embedded in an elastic medium, *Latin American Journal of Solids and Structures* **11**: 659-682.

[39] Mohammadi M., Farajpour A., Goodarzi M., Heydarshenas R., 2013, Levy type solution for nonlocal thermomechanical vibration of orthotropic mono-layer graphene sheet embedded in an elastic medium, *Journal of Solid Mechanics* **5**: 116-132.

[40] Asemi S. R., Farajpour A., Borghei, M., Hassani A. H., 2014, Thermal effects on the stability of circular graphene sheets via nonlocal continuum mechanics, *Latin American Journal of Solids and Structures* **11**: 704-724.

[41] Ghorbanpour Arani A.H., Maboudi M.J., Ghorbanpour Arani A., Amir S., 2013, 2D-magnetic field and biaxiall in-plane pre-load effects on the vibration of double bonded orthotropic graphene sheets, *Journal of Solid Mechanics* **5**: 193-205.

[42] Ghorbanpour Arani A., Amir S., 2013, Nonlocal vibration of embedded coupled CNTs conveying fluid Under thermo-magnetic fields via Ritz method, *Journal of Solid Mechanics* **5**:206-215.

[43] Ghorbanpour Arani A., Kolahchi R., Allahyari S.M.R., 2014, Nonlocal DQM for large amplitude vibration of annular boron nitride sheets on nonlinear elastic medium, *Journal of Solid Mechanics* **6**:334-346.

[44] Anjomshoa A., Shahidi A.R., Shahidi S.H., Nahvi H., 2015, Frequency analysis of embedded orthotropic circular and elliptical micro/nano-plates using nonlocal variational principle, *Journal of Solid Mechanics* **7**:13-27.

[45] Naderi A., Saidi A.R., 2014, Nonlocal postbuckling analysis of graphene sheets in a nonlinear polymer medium, *International Journal of Engineering Science* **81**: 49-65.

[46] Naderi A., Saidi A.R., 2013, Modified nonlocal mindlin plate theory for buckling analysis of nanoplates, *Journal of Nanomechanics and Micromechanics* **4**:130150-130158.

[47] Eringen A.C., Edelen D.G.B., 1972, On nonlocal elasticity, *International Journal of Engineering Science* **10**: 233-248.

[48] Malekzadeh P., Shojaee M., 2013, A two-variable first-order shear deformation theory coupled with surface and nonlocal effects for free vibration of nanoplates, *Journal Vibration and Control* **21**(14): 2755-2772.

[49] Karamooz Ravari M. R., Talebi S. A., Shahidi R., 2014, Analysis of the buckling of rectangular nanoplates by use of finite-difference method, *Meccanica* **49**: 1443-1455.

[50] Karamooz Ravari M.R., Shahidi R., 2013, Axisymmetric buckling of the circular annular nanoplates using finite difference method, *Meccanica* **48**: 135-144.

[51] GreeJ.R, Street R.A., 2007, Mechanical characterization of solution-derived nanoparticle silver ink thin films, *Journal of Applied Physics* **101**: 103529.